World Journal of Microbiology and Biotechnology (2018) 34:7
https://doi.org/10.1007/s11274-017-2391-6

ORIGINAL PAPER

Insights into the genome and proteome of *Sphingomonas paucimobilis* strain 20006FA involved in the regulation of polycyclic aromatic hydrocarbon degradation

M. Macchi[1] · M. Martinez[1] · R. M. Neme Tauil[3] · M. P. Valacco[3] · I. S. Morelli[1,2] · B. M. Coppotelli[1]

Received: 14 July 2017 / Accepted: 2 December 2017

Abstract
In order to study the mechanisms regulating the phenanthrene degradation pathway and the intermediate-metabolite accumulation in strain *S. paucimobilis* 20006FA, we sequenced the genome and compared the genome-based predictions to experimental proteomic analyses. Physiological studies indicated that the degradation involved the salicylate and protocatechuate pathways, reaching 56.3% after 15 days. Furthermore, the strain degraded other polycyclic aromatic hydrocarbons (PAH) such as anthracene (13.1%), dibenzothiophene (76.3%), and fluoranthene. The intermediate metabolite 1-hydroxy-2-naphthoic acid (HNA) accumulated during phenanthrene catabolism and inhibited both bacterial growth and phenanthrene degradation, but exogenous-HNA addition did not affect further degradation. Genomic analysis predicted 126 putative genes encoding enzymes for all the steps of phenanthrene degradation, which loci could also participate in the metabolism of other PAH. Proteomic analysis identified enzymes involved in 19 of the 23 steps needed for the transformation of phenanthrene to trichloroacetic-acid intermediates that were upregulated in phenanthrene cultures relative to the levels in glucose cultures. Moreover, the protein-induction pattern was temporal, varying between 24 and 96 h during phenanthrene degradation, with most catabolic proteins being overexpressed at 96 h—e. g., the biphenyl dioxygenase and a multispecies (2Fe–2S)-binding protein. These results provided the first clues about regulation of expression of phenanthrene degradative enzymes in strain 20006FA and enabled an elucidation of the metabolic pathway utilized by the bacterium. To our knowledge the present work represents the first investigation of genomic, proteomic, and physiological studies of a PAH-degrading *Sphingomonas* strain.

Keywords Genomics · HNA accumulation · Phenanthrene pathway · Proteomics · Strain 20006FA

Introduction

Polycyclic aromatic hydrocarbons (PAH) constitute ubiquitous and serious worldwide pollutants since they are extremely harmful to human health (Vandermeersch et al. 2015) and may drastically affect the biodiversity of natural ecosystems (Zhang et al. 2015). Although several natural and anthropic sources contribute to the release of PAH into the environment, petrochemical activities account for the majority of those compounds contaminating soils and water bodies (Zafra et al. 2017). Microbial degradation is the main process for the ecologic restoration of PAH-contaminated sites (Peng et al. 2008); prokaryotes temporarily change their pattern of gene expression in response to environmental signals, such as sudden spikes in PAH (Fernandez-Luqueno et al. 2011).

The genus *Sphingomonas* includes many strains that are attractive as a result of their diverse environmental

Electronic supplementary material The online version of this article (https://doi.org/10.1007/s11274-017-2391-6) contains supplementary material, which is available to authorized users.

✉ B. M. Coppotelli
bibicoppotelli@gmail.com

[1] Laboratory of Microbial Degradation of Hydrocarbons, Centro de Investigación y Desarrollo en Fermentaciones Industriales, CINDEFI (UNLP; CCT-La Plata, CONICET), Street 50 No 227, 1900 La Plata, Argentina

[2] Comisión de Investigaciones Científicas de la Provincia de Buenos Aires, La Plata, Argentina

[3] IQUIBICEN, FCEN-UBA, Buenos Aires, Argentina

Published online: 06 December 2017

adaptations and their capabilities to degrade xenobiotics and recalcitrant pollutants, including PAH, (Zhao et al. 2017; Khara et al. 2014; Dong et al. 2014; Stolz 2009; Vandermeer and Daugulis 2007). Sphingomonads also make use of original strategies to enhance PAH bioavailability (Fialho et al. 2008; Johnsen and Karlson 2005). Despite the increase in the number or aromatic compounds that are known to be biodegraded by *Sphingomonas*, many critical aspects of the metabolism of those bacteria are still unknown, including the nature of the metabolites in degradation pathways, the evolution and dispersion of degradation-related gene clusters, and the regulatory mechanisms (Zhao et al. 2017).

S. paucimobilis 20006FA was originally isolated from a soil microcosm contaminated with phenanthrene and was selected for its ability to grow on several PAH (e.g., anthracene, phenanthrene, fluoranthene, and dibenzothiophene)—indeed, investigations of its ecological properties have indicated that the strain apparently enhances phenanthrene bioavailability by producing biosurfactants and by adhesion to the phenanthrene crystals (Coppotelli et al. 2010). Studies on pure cultures and contaminated microcosms inoculated with the strain have demonstrated its ability to degrade phenanthrene, though the intermediate metabolite in the phenanthrene-degradation pathway 1-hydroxy-2-naphthoic acid (HNA) was observed to accumulate both in soil and in pure cultures (Coppotelli et al. 2008, 2010). Until now, the regulation of the PAH biodegradation mechanism, the cause of that metabolite accumulation, even the proteomics of the resulting expression, however, have not been studied on *S. paucimobilis* 20006FA. The proteome of an organism provides perspicacious insight into bioremediation-related genes and their regulation (Fulekar and Sharma 2008). The more complete annotation of genomes with the help of proteomic evidence is accordingly paving the way for integrated multiomic approaches in microbiology (Armengaud 2013).

Our aim in the present work was to study the involvement of enzymes or metabolites in the stimulation or inhibition of PAH degradation by strain 20006FA. This objective was pursued through proteomic- and genomic-based approaches along with investigations on the influence of the key metabolite HNA on phenanthrene degradation. The present work represents the first investigation of genomic, proteomic, and physiological studies of a PAH-degrading *Sphingomonas* strain.

Materials and methods

Chemicals

Phenanthrene, anthracene, dibenzothiophene, fluoranthene, HNA, and phthalic acid were purchased from Carlo Erba (Milan, Italy, > 99.5% purity).

Bacterial strain

S. paucimobilis strain 20006FA was isolated from a microcosm whose soil had been artificially contaminated with phenanthrene. That soil had been obtained from an area near La Plata city, Argentina (34°51′24.6″S, 58°06′54.2″W) (Coppotelli et al. 2008).

Bacterial growth conditions

S. paucimobilis 20006FA was grown in either R3 or mineral medium (MM) with glucose, phenanthrene or HNA as described by Coppotelli et al. (2010).

Carbon-source utilization

Growth was tested in sterile liquid minimal medium (LMM) supplemented with phenanthrene or with HNA. Incubation and growth monitoring were performed according to Coppotelli et al. (2010).

PAH degradation

Phenanthrene degradation and HNA formation were analyzed in triplicate at a phenanthrene concentration of 0.84 g L. Cultures were seeded with 2×10^7 colony-forming units (CFUs) mL^{-1} of a 24-h-old prior culture and incubated at 26 °C for 160 h in a rotary shaker at 150 rpm. One no inoculated bioreactor was used as an abiotic control. The cultures were extracted with ethyl acetate and analyzed by reversed-phase high-performance liquid chromatography (HPLC; Coppotelli et al. 2010).

The degradation of anthracene, dibenzothiophene, or fluoranthene, as the sole carbon and energy source was tested in duplicate in sterile LMM. Cultures were incubated at 28 °C, 150 rpm for 7 days.

HNA degradation

The degradation of HNA was measured by HPLC, was performed in triplicate in 50-mL glass bioreactors containing 10 mL of LMM supplemented with 0.05 or 0.14 g L^{-1} of the carbon source.

Statistical analysis

The statistical evaluation of the degradation and counting data were performed by parametric one-way analysis of variance (ANOVA), followed by Tukey's honestly significant difference (HSD) post-hoc test, through the use of the

XLStat-Pro statistical package v7.5.2 (Addinsoft SARL, France).

Whole-genome sequencing, assembly, and annotation

The genome of strain 20006FA was sequenced by the HiSeq 1500 Illumina (2 × 100-bp paired-end reads) sequencing technology. The raw Illumina-sequence data were quality trimmed and filtered by means of the Nextera® XT Illumina protocol. The de-novo assembly of the reads was performed with Illumina's A5-miseq Assembly Pipeline (v. 2.0) platform (Tritt et al. 2012). To annotate the genes, Rapid Annotation with the Subsystem Technology (RAST) server version 2.0 was used (Aziz et al. 2008). A functional analysis of genes was subsequently performed with the KEGG database and a manual curation by means of the genome viewer Artemis (Rutherford et al. 2000) (http://www.sanger.ac.uk/Software/Artemis). To determine each probable coding sequence a BLASTX alignment NCBI database was performed (http://blast.ncbi.nlm.nih.gov). The draft genome sequence of *S. paucimobilis* strain 20006FA was deposited in GenBank Whole-Genome Shotgun Project (listed as WGS) under the Accession Number LYMJ00000000.

Preparation of the cell lysates for proteomic studies

Cells grown in glucose or phenanthrene were harvested for protein analysis in the stationary phase (96 h) or the log phase (24 h). Triplicate cultures were analyzed under each condition.

The preparation of cell lysates was performed according to Pérez Vidakovics et al. (2007). The procedure stated in brief: *S. paucimobilis* strain 20006FA was grown in LMM supplemented with 0.84 g L^{-1} of the corresponding carbon source. Cells from 1000 mL of culture were collected, washed and resuspended in MilliQ water with 5 mM phenylmethylsulfonylfluoride (PMSF) as a protease inhibitor. The cell suspension was disrupted with a Precellys 24-bead beater (Bertin Technologies, location) and solubilized in a solubilization solution containing Amberlite. The protein concentration in the extracts was determined by the Bio-Rad Protein Assay Dye Reagent Concentrate and 2-D Quant Kit (GE Healthcare, Bio-Sciences AB, Uppsala, Sweden).

Proteomic analysis

For isoelectric focussing (IEF), precast 7- and 18-cm pH 4–7 immobilized-pH-gradient (IPG) gels (Immobiline DryStrips, GE Healthcare) were used. Samples were prepared according to Pérez Vidakovics et al. (2007), mixed with rehydration buffer containing Pharmalyte™ pH 3–10, bromophenol blue sodium salt ultrapure, PMSF, and IPG Bufferwith a reducing agent (dithiothreitol; GE Healthcare). The final protein concentration was 2 μg μL^{-1}. The IPGs pH 4–7 were rehydrated with the samples as described (Sánchez et al. 1999).

The IEF was performed with the Ettan IPGphor 3 IEF (GE Healthcare Bio-Sciences) according to Pérez Vidakovics et al. (2007). After the IEF, the IPG strips were treated with equilibration buffer with dithiothreitol (PlusOne) and iodoacetamide (GE Healthcare). Thereafter the IPG strips were mounted on a sodium-dodecyl-sulfate–polyacrylamide gel and overlaid with a 12.5% (w/v) resolving polyacrylamide gel. The separation was carried out at 40 V and 20 °C in a PROTEAN II xi 2-dimensional electrophoresis unit (Bio-Rad, Hercules, CA) connected to a Multitemp II cooling bath (GE Healthcare) for large gels or a Mini PROTEAM Tetra Cell (Bio-Rad, Hercules, CA) for small ones. The gels were stained with Coomassie brillliant blue G-250 the 2-dimensional–gel images captured with Universal Hood II; and spot detection, matching, quantification, and normalization performed by means of the ProteomeWeaver 4.0 program (both from Bio-Rad). The proteins with significant changes in representation were processed for mass-spectrometry (MS) analysis. All the studies were performed in triplicate.

The spots of interest were manually excised and sent to the Mass Spectrometry Facility (CEQUIBIEM) at the School of Exact and Natural Sciences, University of Buenos Aires. A tryptic digestion was performed and the resulting peptides analyzed by ultraviolet matrix-assisted laser desorption ionization-time of flight/time of flight (MALDI-TOF/TOF; UltraflexII BrukerDaltonics). The software used for spectra visualization and tandem-MS (MS/MS) protein identification were Flex Analysis (v. 3.3) and BioTools (Bruker Daltonics), linked to MASCOT (Matrix Science, Boston, MA©2016 http://www.matrixscience.com/) in order to search for the protein-sequence databases listed under the NCBI number. The protein score was calculated as $-10 \times \mathrm{Log}(P)$, where P is the probability at which the observed match was a random event. The proteins identified by MALDI-TOF/TOF were subjected to bioinformatic analysis including similarity searches with predicted 20006FA proteins from the genome in ARTEMIS.

Results

Bacterial growth and the degradation of phenanthrene and other PAH

In order to quantify the phenanthrene degradation and the resulting formation of HNA during strain-20006FA growth, cultures with phenanthrene as the sole carbon and energy source were prepared and chemical analysis performed by HPLC. Figure 1, panels A and B, depict,

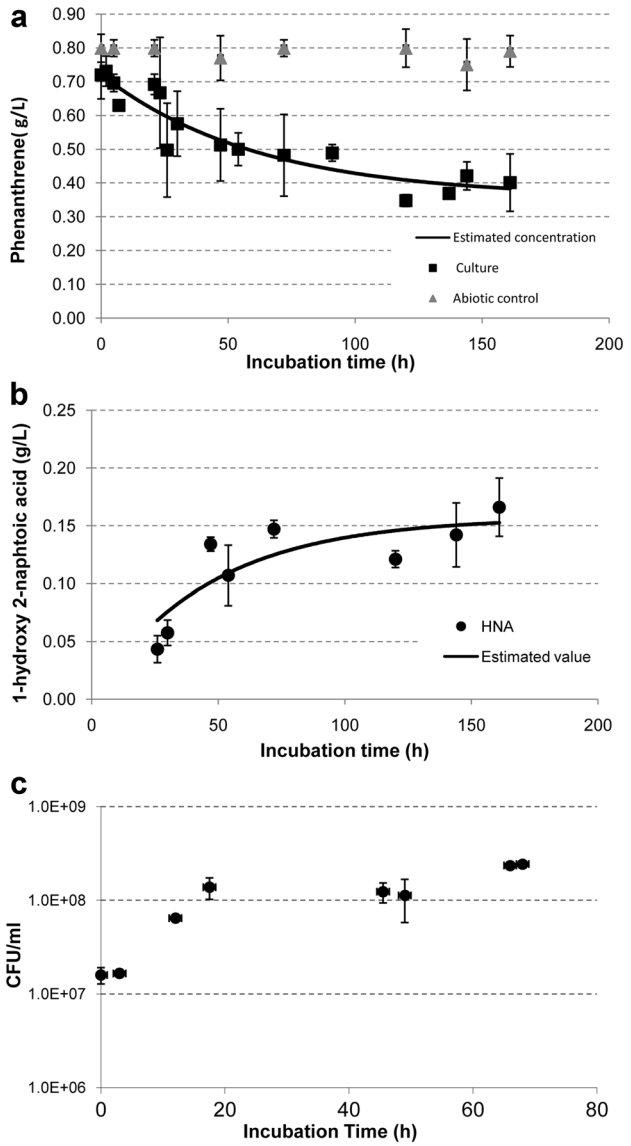

Fig. 1 Concentration of phenanthrene (Panel A) and 1-hydroxy-2-naphthoic acid (HNA; Panel B) and counts of heterotrophic viable bacteria (Panel C) in the strain-20006FA culture growing in LMM with phenanthrene as the sole carbon and energy source (0.84 g L^{-1}) during 161 h of incubation. The results are the means of three biological replicates. The bars represent standard deviations. The mathematical fitting of the curves to growth equations was performed by the SigmaPlot V10, Systat software, Inc., San Jose, CA. In panels A and B, the respective concentrations of phenanthrene (black squares) and HNA (black circles) in g L^{-1} are plotted on the *ordinates* as a function of the inclubation times in h on the *abscissas* for the bacterial cultures or, in Panel A, abiotic controls (gray triangles). The solid curves in panels A and B (Estimated concentrations) are the loci of points representing the functions best fitting the data. In Panel C, the growth of viable bacteria (black circles), expressed as CFUs per mL, is plotted on the *ordinate* as a function of incubation time in h on the *abscissa*

respectively, the phenanthrene remaining and the HNA produced as a function of incubation time in these cultures. Phenanthrene degradation reached 49.1% after 161 h of incubation, but at around 120 h an interruption in that process was recorded.

Phenanthrene biodegradation (Fig. 1, Panel A) was modelled by using a three-parameter logistic function described by the equation: $PHN = P + ae^{-bt}$ (where t is the treatment time and PHN is phenanthrene concentration at time t and a and b are constants that define the curve in accordance with the input raw data). In that equation, the parameter (P) modulates the phenanthrene-elimination rate over time. That parameter could be represented by an influence that depends on PHN concentration and could thus involve at least one of the metabolites accumulated (Fig. 1, Panel B). A decrease in the elimination rate is also indicated in the Supplemental Material (Table S1). A determination of the phenanthrene concentration after 15 days of incubation indicated a final degradation of 59.6%, thus confirming that a progressive decrease in the degradation rate occurred over time. A previous study had demonstrated that this strain could efficiently degrade an initial concentration of 2 g L^{-1} of phenanthrene to 52.9% in 20 days (Coppotelli et al. 2010). Although, in another experiment performed in the present work with cultures initially containing 0.2 g L^{-1} of phenanthrene, the strain was able to attain a degradation of 99% in 15 days. This result may suggest that parameter P depends on the initial phenanthrene concentration.

HNA became detectable from 26 h on and continued to accumulate during the incubation, reaching a concentration of 0.166 g L^{-1} in 161 h. Subsequently, on Day 15, the HNA concentration was *ca.* 0.087 g L^{-1}, thus indicating the occurrence of degradation. For HNA production (Fig. 1, Panel B), the adjustment curve was obtained by using a two-parameter logistic function $Y = a(1 - e^{-bt})$—with an exponential rise to a maximum, where t is the treatment time and a and b are constants that define the curve in accordance with the input raw data.

From the phenanthrene-degradation and HNA-accumulation curves, we clearly observed that the elimination rate of phenanthrene decreased significantly over time (Fig. 1, Panel A), conjointly when the accumulation of intermediate metabolites occurred (i.e., after 24 h; Fig. 1, Panel B). Thereafter, even though the HNA was further degraded, the degradation of phenanthrene did not continue.

Figure 1, Panel C is a plot of the growth of strain 20006FA in those same cultures; growth was determined by CFU counts as a measure of the viable bacteria present at each time point. Under those conditions, the growth rate was 0.146 h^{-1} ($r^2 = 0.995$) and the doubling time 4.72 h. That, at 20 h, the culture entered in a stationary phase while the degradation rate was still high (Fig. 1, Panel A) is indeed noteworthy.

In addition, we determined that the strain was able to degrade anthracene (13.1%) and dibenzothiophene (76.3%), plus a qualitative analysis furthermore demonstrated the production of colored metabolites after 15 days of growth on 0.2 g L^{-1} of fluoranthene. In this regard, a previous publication from our laboratory had documented the metabolization of salicylic acid (Coppotelli et al. 2010); and we now report here that phthalic acid was also metabolized, as judged by an observed and recorded support of bacterial growth (data not shown). Thus indicating that strain 20006FA could be utilizing either the *meta* or the *ortho* pathway for the degradation of phenanthrene (Fig. 3).

HNA—bacterial growth and degradation

In order to study the strain's capability of using HNA as the sole carbon and energy source, cultures in LMM supplemented with HNA at three different concentrations (0.05, 0.14, and 0.3 g L^{-1}) were prepared and monitored to determine microbial growth and remnant-HNA levels. The concentrations were chosen near the values obtained during phenanthrene degradation (Table 1). In the cultures supplemented with 0.05 g L^{-1} of HNA, strain 20006FA grew slowly after a lag phase of 6 h, exhibiting a specific growth rate of 0.148 h^{-1} and a doubling time of 4.72 h. When grown on 0.14 g L^{-1} of HNA, however, the lag phase increased significantly up to 30 h, but the specific growth rate was 0.153 h^{-1} and the doubling time 4.52 h (Fig. 2). At both concentrations of HNA, the medium took on a yellow cast, indicating HNA-ring cleavage. When, strain 20006FA was inoculated in LMM supplemented with 0.3 g L^{-1} HNA, no growth was detected (not shown). That failure could be indicating HNA to be toxic to the strain at that concentration.

The degradation of HNA was determined after 24 h in cultures growing in LMM with HNA as the sole carbon and energy source, at concentrations of 0.05 and 0.14 g L^{-1}. A significantly higher degradation value of 94 ± 9% was obtained in the culture at 0.05 g L^{-1}; compared to that attained at 0.14 g L^{-1}, where 44 ± 8% became degraded. These results, in addition to the considerably longer lag phase observed at 0.14 g L^{-1} of HNA, could indicate an inhibition of cellular metabolism at increasing concentrations of HNA.

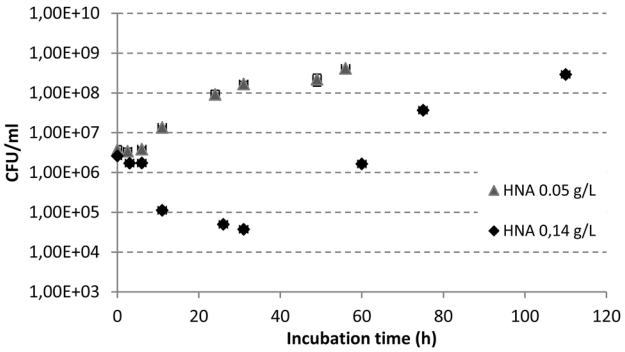

Fig. 2 Cell growth of *S. paucimobilis* 20006FA in LMM with 1-hydroxy-2-naphthoic acid (HNA) as the sole carbon and energy source.In the figure, the growth of viable bacteria (triangles 0.05 g L^{-1}, diamonds, 0.14 g L^{-1}), expressed as CFUs per mL, is plotted on the *ordinate* as a function of incubation time in h on the *abscissa*. The results are means of three biological replicates. The error bars represent standard deviations, but are not shown when of the same dimensions as the symbols

Influence of HNA on phenanthrene-degradation kinetics

In order to investigate if the delay in phenanthrene degradation was caused by an accumulation of HNA, which could inhibit the growth of strain 20006FA; we studied the effect of HNA on phenanthrene degradation. Cultures of the strain in LMM were supplemented with phenanthrene at 0.84 g L^{-1} along with HNA added at a concentration of either 0.05 or 0.14 g L^{-1}. After 24 and 96 h of incubation, the concentrations of HNA and phenanthrene remaining were determined by HPLC. During growth, an orange-to-yellow cast appeared in both media.

Table 1 documents that phenanthrene degradation in both cultures was around 12–14% after 24 h and 41–45% after 96 h. Under these conditions, phenanthrene degradation was not significantly affected by externally added HNA (Table 1), in comparison to the results obtained in the

Table 1 Percent degradation of phenanthrene and concentration of HNA (g L^{-1}) accumulated in cultures of the strain 20006FA growing in LMM with phenanthrene (PHN, 0.84 g L^{-1}) and 1-hydroxy-2-naphthoic acid (HNA) externally added, after 24 and 96 h of incubation

		PHN	PHN + HNA (0.05 g L^{-1})	PHN + HNA (0.14 g L^{-1})
PHN degradation (%)	24 h	15 ± 2	12 ± 4	14 ± 4
	96 h	44 ± 5	45 ± 9	41 ± 4
HNA accumulation (g L^{-1})	24 h	0.07 ± 0.01	0.09 ± 0.01	0.13 ± 0.01
	96 h	0.138 ± 0.007	0.15 ± 0.04	0.19 ± 0.02

Results are means ± standard deviations of three biological replicates

control cultures (PHN), where the degradation was about 15 and 44% after those respective times. After 96 h, HNA had accumulated up to a concentration of 0.15 g L^{-1} in the culture with HNA at 0.05 g L^{-1} and up to a concentration 0.19 g L^{-1} in the culture with HNA at 0.14 g L^{-1}. Since HNA accumulation did not reach values significantly higher than those observed during phenanthrene degradation in cultures with no added HNA (Table 1, column PHN)—i.e., the HNA concentrations measured were less than the sum of the added HNA and the HNA produced in the cultures without HNA addition- this difference could be showing that the cells could be maintaining the concentration under values that would be toxic. Concentrations of HNA within the range 0.15–0.19 g L^{-1} might be suspected to be toxic to the cells of strain 20006FA. Despite the decline in phenanthrene-degradation rate observed (Fig. 1, Panel A and supplementary Table S1), the HNA concentration remained within a constant range (around 0.15 g L^{-1}) that allowed a continuation of phenanthrene degradation over time.

Genomic analysis

In-silico analysis of the genome of *S. paucimobilis* 20006FA revealed a high number of open-reading frames (ORFs) predicted to encode enzymes for aromatic-hydrocarbon degradation (Tables 2, 3). Table 2 lists the general features of the genome. A genome sequencing yielded 144 scaffolds along with 4862 predicted coding genes. The strain possesses multiple ORF homolog for enzymes with similar functions that are implicated in PAH degradation; they are distributed throughout the bacterial chromosome, and are not organized in gene clusters. On the basis of this analysis, we have predicted 126 putative genes encoding enzymes for all the steps in the degradation of phenanthrene to acetyl-CoA and succinyl-CoA. The gene products of selected ORFs that were likely to be involved in both the *ortho* and the *meta* phenanthrene-degradation pathways, are summarized in Table 3. The steps in the scheme of Fig. 3 in which these enzymes could be implicated are also indicated in Table 3. The ORFs that were confirmed by the proteomic analysis described below to be coding for the enzymes involved in the degradation steps are shadowed in gray.

Table 2 General genome feature of *S. paucimobilis* strain 20006FA

Genome feature	
Size (bp)	5,409,713
GC content (%)	64.3
Gene number	5077
Protein-coding sequences (CDSs)	4882
RNA gene number	56
rRNA gene number	4
tRNAs gene number	49
ncRNAs gene number	3
Pseudogene number	115

CDS coding sequence, *INSDC* International Nucleotide Sequence Database Collaboration, *ncRNAs* noncoding RNAs

We found six ORFs that shared a significant identity with components of ring-hydroxylating dioxygenases that catalyze the initial step of phenanthrene degradation and the conversion of specific intermediate metabolites. Several genes are a flanked by, transposon or transposon-like sequences. A particular region, corresponding to scaffold number 19, has a high frequency of ORFs for PAH-degrading enzymes. This region exhibits a 92% similarity to and a 76% coverage of the sequence of plasmid pNL1 from *NovoSphingobium (*originally *Sphingomonas) aromaticivorans* F199 (Romine et al. 1999).

Proteomic analysis

In order to study the effect of phenanthrene on the cellular response, the proteome of *S. paucimobilis* 20006FA grown in batch cultures under two different conditions—utilizing either glucose or phenanthrene as the sole carbon source—were analyzed by two-dimensional gel electrophoresis.

Proteomic background of biodegradation

The growth curves of strain 20006FA on glucose or phenanthrene as the sole carbon source indicated that the cultures reached the stationary phase of growth after 96 h (Supplemental Material Fig. S1). At that time, quantitative analysis of biodegradation (Fig. 1) revealed that more than 40% of the initial phenanthrene had been removed and the principal derivative HNA had reached a concentration of *ca.* 0.13 g L^{-1}. On the basis of the growth phase and degree of phenanthrene degradation illustrated in Fig. 1, we established the optimal culture conditions for comparative proteome analysis of strain 20006FA after 96 h of growth. Upon consideration of the kinetics of phenanthrene-derivative formation, we determined the optimal culture conditions for comparative proteome analysis of strain 20006FA with respect to phenanthrene degradation to be at *ca.* 24 and 96 h.

Proteomic response to phenanthrene

The proteins obtained from the bacterial lysates of cultures containing glucose or phenanthrene as the sole carbon source were analyzed by two-dimensional-electrophoresis in order to identify the enzymes expressed during phenanthrene degradation. Accordingly, under those conditions, the electrophoreses resolved *ca.* 250 protein spots (Fig. 4). The differentially expressed protein spots were then excised and analyzed by MALDI-TOF/TOF (MS/MS). The MASCOT

Table 3 Predicted enzymes belonging to PAH degradation pathways in *S. paucimobilis* strain 20006FA strain, obtained with the RAST server and KEGG database and curated by the National Center for Biotechnology Information (NCBI) database

Steps of degradation pathway	Enzymes predicted from the Upper and Lower pathway of PAH degradation in the strain *Sphingomonaspaucimobilis*20006FA	ORFs*	IdentifiedProteins (2D-PAGE**)
1, 10	aromatic-ring-hydroxylatingdioxygenase alpha and beta subunit (EC 1.14.12.-)	4	J L
1, 3, 7	2,3-dihydroxybiphenyl 1,2-dioxygenase (EC 1.13.11.39)	1	B 29
1, 3, 10	biphenyl 2,3-dioxygenase (EC 1.14.12.18)	1	B 29 J
2, 11, 18	1,2-dihydroxycyclohexa-3,5-diene-1-carboxylate dehydrogenase (EC 1.3.1.25)	1	31
2, 11, 18	1,6-dihydroxycyclohexa-2,4-diene-1-carboxylate dehydrogenase (EC 1.3.1.25)	1	31
4, 13	maleylacetoacetateisomerase (EC 5.2.1.2)	1	
5, 12, 17	4-carboxymuconolactone decarboxylase (EC 4.1.1.44)	1	11
5	carboxymuconolactonedecarboxylase	4	11
5, 8, 17	4-hydroxy-2-oxovalerate aldolase (EC 4.1.3.39)	3	6, 7
6, 18	acetaldehydedehydrogenase (EC 1.2.1.10)	4	31 27 C
8	carboxymuconolactonedecarboxylase	5	11
8	4-oxalocrotonate decarboxylase	4	11
9	aldehydedehydrogenase (EC 1.2.1.3)	12	C 27
9	2-hydroxymuconic semialdehydedehydrogenase (EC 1.2.1.60)	2	C 27
10	benzoate 1,2-dioxygenase alpha and beta subunit (EC 1.14.12.10)	1	L
10	anthranilate 1,2-dioxygenase small subunit (EC 1.14.12.1)	2	L
13, 15, 20	homogentisate 1,2-dioxygenase (EC 1.13.11.5)	1	8 B 29
14, 19	ciclohexanonemonooxygenase (EC 1.14.13.22)	1	
16	muconolactone delta-isomerase (EC 5.3.3.4)	1	
16, 13	muconatecycloisomerase (EC 5.5.1.1)	1	
17	2-keto-4-pentenoate hydratase (EC 4.2.1.80)	2	10
18	5-carboxymethyl-2-hydroxymuconate semialdehydedehydrogenase (EC 1.2.1.60)	2	27
21	salicylatehydroxylase (EC 1.14.13.1)	1	
22, 23	catechol 2,3-dioxygenase (EC 1.13.11.2)	2	8
22	catechol 1,2-dioxygenase (EC 1.13.11.1)	2	8
***	(2Fe-2S)-bindingprotein	15	M

*ORF: of open-reading frames for that protein in the genome. **2D-PAGE, two-dimensional polyacrylamide-gel electrophoresis.

***: Component of the dioxygenase complexes that act in different steps of the pathway.

The ORFs that were confirmed by the proteomic analysis are shadowed in gray

program and the database of the translated proteins of the strain-20006FA genome were used for protein identification. The protein profiles revealed an overexpression of multiple structural genes belonging to the phenanthrene catabolic pathway in the phenanthrene-grown cultures compared to the corresponding profile of the control cultures (the glucose-grown cells), with the more pronounced differences being demarcated by the black rectangle in Fig. 4. Table 4 details the identification of those proteins.

A comparison of the gels yielded 17 potentially relevant protein spots—proteins differentially expressed under the influence of the presence of PAH as the sole carbon source—from which spots 15 different proteins could be identified by mass spectrometry (marked with gray circles in Fig. 4). Those identifications revealed that all the indicated proteins had a similarity to those of other strains of *Sphingomonas*. The latter proteins included one NahA1f (naphthalene dioxygenase alpha subunit; Spot 29), one catechol 2,3-dioxygenase (Spot 8), one 2,3-dihydroxybiphenyl 1,2-dioxygenase (Spot B), two glutathione *S*-transferases (spots U and 24), and enzymes for the lower metabolic pathway—e. g., 2-hydroxymuconic semialdehyde hydrolase (spots 12, 17 and 26), 4-oxalocrotonate decarboxylase (Spot 11), along with others (Table 4).

Bacterial growth on phenanthrene thus produced an upregulation of proteins involved in that compound's degradation, including enzymes from both the upper (spots 6, 7, 11, 27, 29, 31, B) and the lower (spots 8, 10, 12, 17, 26) catabolic pathways along with other enzymes involved in cellular detoxification (spots U and 24).

Proteomics of the cells during phenanthrene degradation

Because a gel of 18 cm resulted in a spreading-out of spots within a sample that, through attenuation, prevented the visualization of the proteins at low concentrations, we switched to gels of 7 cm to more clearly observe the differences between phenanthrene cultures under two conditions. We compared the profiles of protein expression at two time points during phenanthrene degradation and

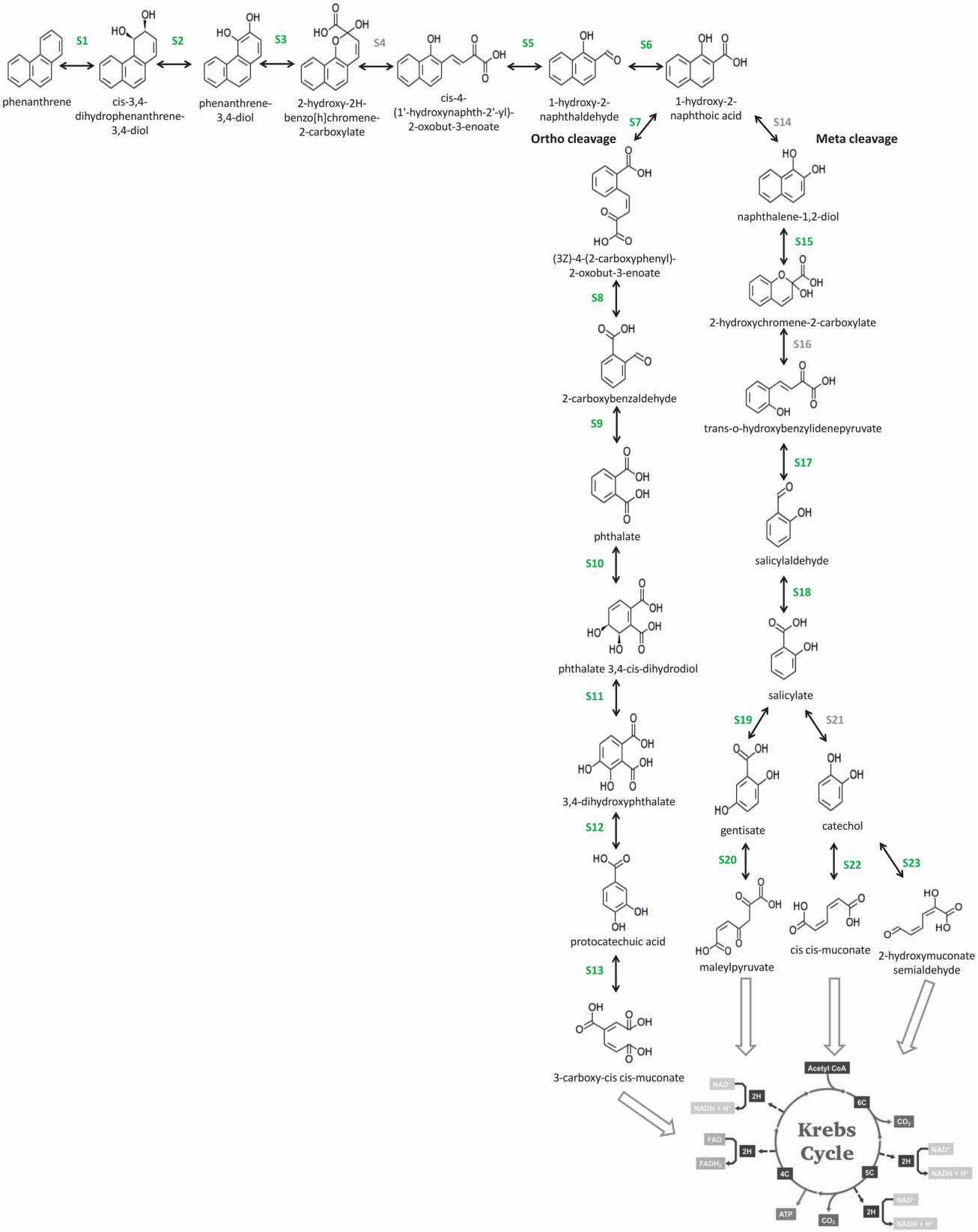

Fig. 3 The reconstructed phenanthrene-degradation pathway based on the genome and proteome analyses on *S. paucimobilis* 20006FA. The Ss over the conversion arrows indicate step numbers

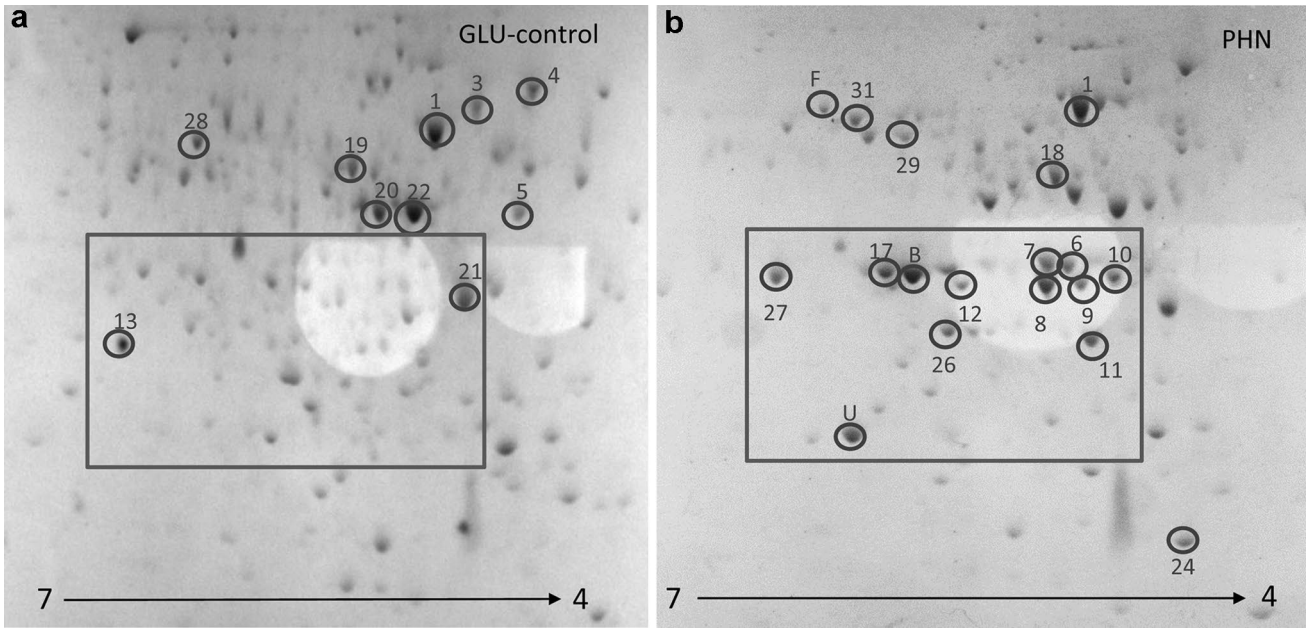

Fig. 4 Two-dimensional (18-cm) electrophoresis gels of soluble fractions of (Panel 1) GLU- and (Panel 2) PHN-grown cultures of *S. paucimobilis* 20006FA after 96 h of incubation. The spots marked were analyzed by MALDI-TOF/TOF. The black circles indicate the proteins identified

Table 4 Summary of Mascot search results

Spot label	Protein description	GLU	PHE 96 h	PHE 24 h	NCBI no.	Theoretical migration		Score	Coverage	CDS	
						Mr (Da)	PI		(%)	Start	Stop
1	chaperonin GroEL [Sphingomonas sp. SKA58]	✓	✓	✓	gi|94497512	52427	5.15	138	36	2981349	2983001
3	ribosomal protein S1 [Sphingomonas sp. SKA58]	✓			gi|94497990	61616	5.01	89	32	4728086	4729816
4	Chaperonine DnaK [Sphingomonas sp. SKA58]	✓			gi|94496879	67507	4.77	173	7	2535305	2537254
5	DNA-directed RNA polymerase, alpha subunit [Sphingomonas sp. SKA58]	✓			gi|94496225	37939	4.94	115	28	4586713	4587807
13	3-hydroxybutyrate dehydrogenase [Sphingomonas wittichii RW1]	✓			gi|148556334	27479	6.51	150	26	1586603	1587706
19	dihydrolipoamide succinyl transferase [Sphingomonas sp. SKA58]	✓			gi|94496913	43776	5.33	68	5	4137048	4138325
21	Electron-transfer flavoprotein alpha-subunit, (ETFLS) [Sphingomonas sp. SKA58]	✓			gi|94498756	31569	4.98	237	10	4215886	4216854
A	succinyl-CoA synthetase subunit alpha [Sphingobium]		✓		gi|490321670	29976	5.51	62	5	4141180	4142103
B	2,3-dihydroxybiphenyl 1,2-dioxygenase [Sphingobium chungbukense]		✓	✓	gi|4007893	33421	5.54	120	10	3496244	3497146
F	ATP synthase subunit alpha [Sphingomonadaceae]		✓		gi|294012668	54727	5.60	188	40	4995782	4997329
J	ring-hydroxylating dioxygenase large subunit [uncultured bacterium]		✓		gi|406718203	35464	5.64	164	12	3546301	3547812
L	BphA1d (Biphenyl dioxygenase large subunit)[Sphingomonas sp. LH128]		✓		gi|158346884	47324	5.57	173	19	3491834	3493185
M	MULTISPECIES: (2Fe-2S)-binding protein [Sphingomonadaceae]		✓		gi|496103618	47477	5.31	92	35	3498018	3499292
P	Ubiquinone-biosynthesis protein UbiD [Novosphingobium]		✓	✓	gi|500246287	52942	5.17	103	10	3510553	3512076
6	4-hydroxy-2-oxovalerate aldolase [Sphingomonas chungbukensis]		✓	✓	gi|4007416	37010	5.10	181	42	3483998	3485104
7	Putative 2-hydroxy-benzylpyruvate aldolase [Sphingomonas sp. P2]		✓	✓	gi|28971850	35759	5.12	187	15	3466433	3467443
8	catechol 2,3-dioxygenase [Sphingomonas agrestis]		✓	✓	gi|151128	34543	5.11	337	82	3488745	3489686
10	2-hydroxypent-2,4-dienoate hydratase [Sphingomonas chungbukensis]		✓	✓	gi|2316027	28142	5.09	354	32	3485987	3486793
11	4-oxalocrotonate decarboxylase [Sphingomonas chungbukensis]		✓	✓	gi|4091975	27280	5.02	147	57	3483226	3484017
12	2-hydroxymuconic semialdehyde hydrolase [Sphingobium chungbukense]		✓		gi|1923245	31340	5.40	178	63	3489687	3490640
17	XylF (2-hydroxymuconic semialdehyde hydrolase) [Sphingomonas sp. LH128]		✓	✓	gi|158346887	30953	5.50	311	26	3489687	3490640
18	translation elongation factor [Sphingomonas sp. SKA58]	✓	✓	✓	gi|94498474	42980	5.21	85	31	2755441	2756637
24	glutathione S-transferase [Sphingobium chungbukense]		✓	✓	gi|158346886	21470	5.34	156	51	3490706	3491353
26	2-hydroxymuconic semialdehyde hydrolase [Sphingobium chungbukense]		✓	✓	gi|1923245	27695	5.28	178	87	3480363	3481265
27	acetaldehyde dehydrogenase (acylating) [Sphingobium chungbukense]		✓		gi|4007415	33138	5.64	241	80	3485026	3486093
28	dihydrolipoamide dehydrogenase [Sphingobium japonicum UT26S]	✓	✓		gi|294012415	48666	5.68	148	32	4135260	4136663
29	ring-hydroxylating dioxygenase large subunit [uncultured bacterium]		✓		gi|158346890	52139	5.47	162	39	3546301	3547509
31	benzaldehyde dehydrogenase [Sphingobium chungbukense]		✓		gi|6136053	54650	5.98	270	51	3481195	3482736
C	acetaldehyde dehydrogenase [Sphingobium sp. C100]		✓	✓	gi|566043422	34452	5.28	86	34	3485026	3485955
R	glutamate-cysteine ligase, partial [Xanthomonas euvesicatoria]			✓	gi|733444971	27612	5.29	119	16		
U	BphK (glutathione S-transferase) [Sphingomonas sp. LH128]		✓	✓	gi|2316034	21518	5.52	148	63	3490706	3491353

*The list indicates the proteins identified (high score and/or high sequence coverage) found in two-dimensional–electrophoresis gels of cultures in GLU, PHN 24 h and PHN 96. The gray-shadowed: proteins belong to the phenanthrene degradation pathway (24 and 96 h). The unshadowed proteins belong to central metabolism. ✓ indicates proteins present under each condition. NCBI, National Center for Biotechnology Information; CDS, coding sequence

The gray-shadowed rows indicate proteins that belong to the phenanthrene degradation pathway

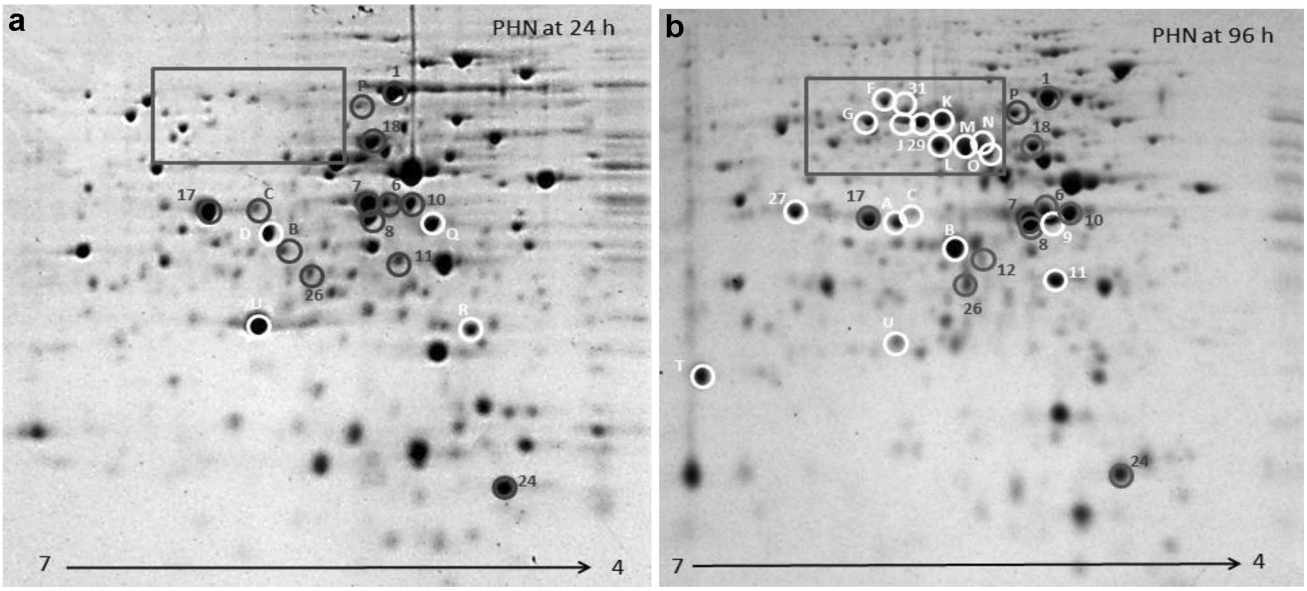

Fig. 5 Two-dimensional (7-cm) electrophoresis gels of soluble fractions PHN cultures of *S. paucimobilis* 20006FA after (Panel A) 24 and (Panel B) 96 h of culture. The spots marked were analyzed by MALDI-TOF/TOF: The black circles indicate the proteins present under both conditions, the white circles the overexpressed proteins under each condition

recorded the following differences (Fig. 5). Certain overexpressed proteins were found in the cultures at 24 h relative to the levels present at 96 h; but, of the former, only two could be identified, a glutamate–cysteine ligase (Spot R) and a glutathione *S*-transferase (GST; Spot U; Fig. 5; Table 4).

Whereas proteins belonging to the phenanthrene degradation pathway were already expressed at 24 h, many others were overexpressed at 96 h (spots encircled in white within the black rectangle in Fig. 5). The latter included a 2,3-dihydroxybiphenyl 1,2-dioxygenase (Spot B), the large subunit of a biphenyl dioxygenase (BphA1; Spot L), the large subunit of a ring-hydroxylating dioxygenase (Spot J), and multispecies—i. e., the (2Fe–2S)-binding protein (Spot M; Fig. 5; Table 4). We found enzymes for the first steps of the phenanthrene pathway at both time points. While only one initial dioxygenase (Spot B) was present at 24 h, three overexpressed dioxygenases became detectable at 96 h (spots J, L, and 29) in addition to the (2Fe–2S)-binding protein (Spot M), the alpha subunit of a succinyl-CoA synthetase (Spot A) and a ubiquinone-biosynthesis protein UbiD (Spot P; Tables 3, 4). Other enzymes catalyzing the first steps of the pathway were likewise overexpressed at 96 h (spots 12, 27, and 31).On the contrary, many of the enzymes catalyzing the lower steps of the pathway were expressed at both those time points during phenanthrene degradation (e.g., spots 6, 7, 8, 10, 11 and C; Fig. 5; Table 4).

Such observations probably result from a complex system of regulation controlling the expression of the catabolic genes involved in PAH degradation in strain 20006FA that involves an increasing rate of gene transcription with the time of exposure to the contaminant.

As illustrated in Table 4 and Figs. 4 and 5, by this approach we were able to identify the enzymes required for 19 of the 23 steps of the complete phenanthrene-degradation pathway (Fig. 3). These proteins included 10 enzymes involved in the degradation of phenanthrene to HNA; 10 in the degradation of HNA to salicylate (i.e., the *meta* pathway); 11 in the degradation of HNA to protocatechuate (i.e., the *ortho* pathway); and 3 that could be responsible for the transformation of salicylate to acetyl coenzyme A (acetyl-CoA) and succinyl-CoA. These results agree well with the ORFs assigned in the genomics analysis listed in Table 3, thus suggesting that those loci could be undergoing an induced transcription to give rise to proteins.

Discussion

Our previous studies on *S. paucimobilis* strain 20006FA, demonstrated that bacterium to be a suitable candidate for bioaugmentation in soil because the strain could efficiently degrade phenanthrene to HNA and salicylic acid as major metabolic products (Coppotelli et al. 2010). Since the accumulation of metabolites occurs during degradation, we attempted to find any regulation that could clarify that point.

In this work, the draft genome sequence enabled the identification of the genes related to phenanthrene metabolism in strain 20006FA, although the information on the genome is far from complete. We undertook an approach involving

physiological and proteomic studies in order to improve our understanding of the biological process. The proteomics determined substantiated the predictive information obtained by genomics analysis and enabled the elucidation of the metabolic pathway utilized by the bacterium.

Physiological studies showed that strain 20006FA possessed enzymes that degraded PAH such as anthracene, dibenzothiophene, and fluoranthene. When the strain was grown in liquid MM with phenanthrene as the sole carbon source, the bacterium could efficiently degrade 52.9% of the phenanthrene present at an initial concentration of 2 g L^{-1} in 20 days (Coppotelli et al. 2010), 59.6% of phenanthrene at 0.84 g L^{-1} in 15 days, and more than 99% at 0.2 g L^{-1} in 15 days. These results agree with Waigi et al. (2015), who have also observed that the concentration of a contaminant like phenanthrene is known to play a critical role in bacterial growth and as consequence, could produce lower rates of degradation at higher concentrations of pollutant.

The rate of degradation observed could be related to the accumulation of the intermediate metabolites. During the degradation occurring at 0.84 g L^{-1}, an accumulation of the intermediate acid HNA was observed (Fig. 1) along with a concomitant decrease in the phenanthrene-degradation rate. We postulated that the presence of HNA could have been inhibiting phenanthrene degradation by a possible negative-feedback mechanism or, alternatively, may have acted as a toxic compound for the strain. It was resolved in cultures with HNA present as the sole carbon source where an increase in the lag phase occurred along with an inhibition of cell growth at increasing concentrations of HNA (Fig. 2). Other authors had also observed that an accumulation of phenanthrene metabolites might lead to a toxicity that affected cell growth (Yuan et al. 2000; Zhao et al. 2008).

The enzyme salicylate hydroxylase catalyzes both the salicylate hydroxylation and the conversion of 1-hydroxy-2-naphthoate to 1,2-dihydroxynaphthalene (Cho et al. 2005). The latter reaction is a key step in the biodegradation of phenanthrene by Gram-negative bacteria. Jouanneau et al. (2007) purified the enzyme and found that 1-hydroxy-2-naphthoate was not a substrate, but rather induced NADH oxidation at a high rate in an uncoupled reaction that, in turn, might inhibit PAH degradation. They observed an inhibition of salicylate hydroxylation by the presence of 1-hydroxy-2-naphthoate and postulated that inhibition could be deleterious to bacterial cells growing on PAH. In our studies, on cultures with phenanthrene where HNA was added externally, no significant additional accumulation of HNA was observed at either concentration investigated (Table 1). This result indicated that the presence of exogenous HNA did not inhibit the degradative ability of the cells. Transport mechanisms have to be taken into consideration when designing superior biocatalysts for bioremediation purposes (Pieper and Reineke 2000). Since xenobiotic compounds are usually transported by specialized systems (Pao et al. 1998), a saturation of such a transporter could be the cause of an inhibition of the uptake of HNA into the cytoplasm.

The draft genome analysis of *S. paucimobilis* 20006FA predicted the existence of a complete catabolic pathway for phenanthrene (Table 3; Fig. 3). *S. paucimo*bilis 20006FA possesses multiple ORFs for enzymes implicated in PAH degradation that are highly dispersed throughout the genome, as had been observed for other sphingomonads (Zhao et al. 2017; Demaneche et al. 2004). The arrangement of degradative genes in sphingomonads is complex with genes scattered across several gene clusters in contrast to the coordinately regulated organized operonic structure of genes in *Burkholderia, Pseudomonas* and *Rhodococcus* (Khara et al. 2014).

An analysis of the genome sequence indicated that at least one ORF could be assigned to each of the enzymatic steps required for the complete phenanthrene-degradation pathway (Table 3; Fig. 3). The genes could also be involved in the degradation of other PAH, as revealed by physiological studies and simple sequence comparisons. The phenanthrene degradation assay (Fig. 1a) and the analysis of the assembled draft genome the strain revealed that this strain could be considered a single generalist that can fully metabolize the carbon source (Festa et al. 2017).

The catabolic versatility of the enzymes used in PAH degradation by sphingomonad strains have been well established: these bacteria exhibit a flexible organization of genes (different combinations with some conserved gene clusters), which plasticity aids in prompt and efficient adjustments to the presence of novel compounds in contaminated terrestrial sites (Basta et al. 2005).

In *S. paucimobilis* 20006FA as in other sphingomonads (Zhao et al. 2015, 2017) the gene clusters are flanked by plasmid-derived insertion sequences that promote the transfer of genes and provide peripheral metabolic functions. The transfer of large plasmids responsible for the degradation of PAHs has been observed in *Sphingomonas* and *Sphingobium* strains (Basta et al. 2004). Other studies on PAH-degrading strains indicated that certain catabolic genes were located on plasmids (Basta et al. 2005). The sequence similarities observed between the strain 20006FA *phn* genes (phenanthrene-catabolic genes) and the corresponding *bph* genes (biphenyl-catabolic genes) found on plasmid pNL1, seem to imply that the gene arrangement was the same. Moreover, several PAH-induced proteins found in strain-20006FA cell extracts displayed strong sequence similarity to the gene products found in the pNL1 plasmid—including *xylQ* (acetaldehyde dehydrogenase*), nahE* (a putative 2-hydroxybenzylpyruvate aldolase), and *bphK* (glutathione *S*-transferase). The gene clusters *bph* and *xyl*, also present in the plasmid pNL1 had been found in the genomes of other PAH-degrading strains belonging to the genus *Sphingomonas* and

Sphingobium such as *Sphingobium* sp. C100 (Dong et al. 2014) and *Sphingobium yanoikuyae* B1 (Zhao et al. 2015, 2017).

The predicted enzymes—such as the ring-hydroxylating dioxygenase alpha and beta subunits, 2,3-dihydroxy-biphenyl-1,2-dioxygenase, and anthranilate 1,2-dioxygenase (Table 3)—could attack phthalate; while enzymes like benzoate 1,2-dioxygenase alpha and beta subunit and biphenyl 2,3-dioxygenase (Table 3) could act on protocatechuate and even be involved in the *ortho* pathway for phenanthrene degradation. This supposition was confirmed with the physiological observations of strain 20006FA growing on *o*-phthalate as the sole carbon source, as mentioned above.

Most of the genes in the PAH-degrading sphingomonads have been annotated through different approaches—such as through cloned DNA fragments and target-protein expression or by functional evidence (Demaneche et al. 2004)—but a proteomic elucidation of the pathway has never been realized. Until the present work, only one PAH-degrading *S. paucimobilis* (EPA 505; Desai et al. 2008; Story et al. 2004) had been fully sequenced (WGS: JFYY00000000), but no proteomic studies had been undertaken on that strain.

The proteomic data obtained in this work enabled the identification of enzymes catalyzing 19 steps required for the degradation of phenanthrene to intermediates entering the TCA cycle in strain 20006FA. The results of phenanthrene-degradation experiments and the determination of protein expression (Figs. 1, 3; Table 4) indicated that specific catabolic enzymes were differentially regulated during growth on phenanthrene in comparison to those in the bacterium grown on glucose. Those enzymes allowed the strain to follow the *meta*- as well as the *ortho*-cleavage pathway for phenanthrene degradation, as had been reported for other sphingomonads (Cerniglia and Yang 1984; Gibson 1984).

The pattern of protein induction varied between 24 and 96 h of exposure to PAH. A higher number of enzymes for the upper metabolic pathway were overexpressed at 96 h (Fig. 5; Table 4). Although most of the phenanthrene-pathway enzymes were overexpressed at 96 h, the HNA nevertheless accumulated (Fig. 1). Enzymes that could act in the production of HNA (Step 6 of the pathway)—such as the ones corresponding to acetaldehyde dehydrogenase (Spot C), expressed at either 24 or 96 h, or the acetaldehyde and benzaldehyde dehydrogenases (spots 27 and 31), overexpressed at 96 h—suggest that regulation could occur at this stage. That a higher number of dioxygenase enzymes were overexpressed at 96 h (spots B, J, L, M, 8, 29) compared to those at 24 h (spots B, 8) suggests that the regulation of the phenanthrene degradation rate occurs at the transcriptional level. In the degradation of PAH, the genes involved in the same pathway for a given aromatic compound are specifically regulated at the transcriptional level by regulatory proteins that are activated by aromatic compounds (Fernández et al. 1994). Based on the prediction of regulation, it has already been suggested that multiple inducers are required for the expression of aromatic catabolic enzymes in sphingomonads. The regulation of genes for various aromatic degradation in sphingomonads is quite complex (Khara et al. 2014).

The fact that at 96 h most of the phenanthrene-pathway enzymes were overexpressed could also be an indicator of the regulation of enzymatic activity, because a regulation by negative-feedback can also occur since despite the increased enzymatic expression (Fig. 5; Table 4), phenanthrene degradation rate did not increase (Fig. 1).

Despite not finding the salicylate hydroxylase in the proteome results, we included that enzyme in the degradation pathway of Fig. 3 based on the genetic location and functional confirmation of the enzymatic activity, since salicylate was catalysed by this strain (Coppotelli et al. 2010). The enzyme GST was found overexpressed in phenanthrene-containing cultures in comparison to cultures with glucose. The upregulation of GST had also been reported for other PAH-stressed *Sphingomonas* strains (Cavalca et al. 2007; Xia et al. 2005) and is in agreement with the production of oxidative damage by oxygenases involved in the degradation of xenobiotics (Favaloro et al. 2000).

Conclusions

The present work represents the first investigation of genomic, proteomic, and physiological studies of the strain *S. paucimobilis* 20006FA. A large number of genes coding for dioxygenase enzymes were present in the genome suggesting a considerable aromatic-biodegradation potential. Integration of studies indicated that the degradation occur via the salicylate and protocatechuate pathways. In the proteomic studies, we identified enzymes of the phenanthrene-degradation pathway of the strain that enabled the construction of a complete pathway of phenanthrene degradation. Many of those proteins were expressed differentially during phenanthrene degradation or when compared with those from cultures with glucose as the sole carbon and energy source, thus suggesting that a regulation occurs at those loci. The first hints on regulation of the expression and activity of PAH degradative enzymes were found. The results will facilitate a more complete understanding of the biodegradation mechanism of the strain, which knowledge is essential for achieving a successful removal of the pollutant.

Acknowledgements This research was partially supported by the Agencia Nacional de Promoción Científica y Tecnológica (PICT 2013-0103 and 2010-1983). Macchi M. has a doctoral fellowship supported by CONICET. Morelli I.S. is a research member of CIC-PBA. Coppotelli B.M. and Valacco MP are research members of CONICET. Dr.

Donald F. Haggerty, a retired academic career investigator and native English speaker, edited the final version of the manuscript.

References

Armengaud J (2013) Microbiology and proteomics, getting the best of both worlds! Environ Microbiol 15(1):12–23

Aziz RK, Bartels D, Best AA, DeJongh M, Disz T, Edwards RA, Formsma K, Gerdes S, Glass EM, Kubal M (2008) The RAST server: rapid annotations using subsystems technology. BMC Genom 9(1):75

Basta T, Keck A, Klein J, Stolz A (2004) Detection and characterization of conjugative degradative plasmids in xenobiotic-degrading *Sphingomonas* strains. J Bacteriol 186(12):3862–3872

Basta T, Buerger S, Stolz A (2005) Structural and replicative diversity of large plasmids from sphingomonads that degrade polycyclic aromatic compounds and xenobiotics. Microbiology 151(Pt 6):2025–2037

Cavalca L, Guerrieri N, Colombo M, Pagani S, Andreoni V (2007) Enzymatic and genetic profiles in environmental strains grown on polycyclic aromatic hydrocarbons. Antonie Van Leeuwenhoek 91(4):315–325

Cerniglia C, Yang S (1984) Stereoselective metabolism of anthracene and phenanthrene by the fungus *Cunninghamella elegans*. Appl Environ Microbiol 47:119–124

Cho O, Choi KY, Zylstra GJ, Kim YS, Kim SK, Lee JH, Sohn HY, Kwon GS, Kim YM, Kim E (2005) Catabolic role of a three-component salicylate oxygenase from *Sphingomonas yanoikuyae* B1 in polycyclic aromatic hydrocarbon degradation. Biochem Biophys Res Commun 327(3):656–662

Coppotelli BM, Ibarrolaza A, Del Panno MT, Morelli IS (2008) Effects of the inoculant strain *Sphingomonas paucimobilis* 20006FA on soil bacterial community and biodegradation in phenanthrene-contaminated soil. Microb Ecol 55(2):173–183

Coppotelli BM, Ibarrolaza A, Dias RL, Del Panno MT, Berthe-Corti L, Morelli IS (2010) Study of the degradation activity and the strategies to promote the bioavailability of phenanthrene by *Sphingomonas paucimobilis* strain 20006FA. Microb Ecol 59:266–276

Demaneche S, Meyer C, Micoud J, Louwagie M, Willison JC, Jouanneau Y (2004) Identification and functional analysis of two aromatic-ring-hydroxylating dioxygenases from a *Sphingomonas* strain that degrades various polycyclic aromatic hydrocarbons. Appl Environ Microbiol 70(11):6714–6725

Desai AM, Autenrieth RL, Dimitriou-Christidis P, McDonald TJ (2008) Biodegradation kinetics of select polycyclic aromatic hydrocarbon (PAH) mixtures by *Sphingomonas paucimobilis* EPA505. Biodegradation 19 (2):223–233

Dong C, Bai X, Lai Q, Xie Y, Chen X, Shao Z (2014) Draft Genome sequence of *Sphingobium* sp. strain C100, a polycyclic aromatic hydrocarbon-degrading bacterium from the deep-sea sediment of the Arctic Ocean. Genome Announc 2(1):e01210–e01213

Favaloro B, Tamburro A, Trofino M, Bologna L, Rotilio D, Heipieper H (2000) Modulation of the glutathione *S*-transferase in Ochrobactrum anthropi: function of xenobiotic substrates and other forms of stress. Biochem J 346(2):553–559

Fernandez S, Shingler V, De Lorenzo V (1994) Cross-regulation by XylR and DmpR activators of *Pseudomonas putida* suggests that transcriptional control of biodegradative operons evolves independently of catabolic genes. J Bacteriol 176(16):5052–5058

Fernandez-Luqueno F, Valenzuela-Encinas C, Marsch R, Martinez-Suarez C, Vazquez-Nunez E, Dendooven L (2011) Microbial communities to mitigate contamination of PAHs in soil-possibilities and challenges: a review. Environ Sci Pollut Res Int 18(1):12–30

Festa S, Coppotelli BM, Madueño L, Loviso CL, Macchi M, Tauil RMN, Valacco MP, Morelli IS (2017) Assigning ecological roles to the populations belonging to a phenanthrene-degrading bacterial consortium using omic approaches. PLoS ONE 12(9):e0184505

Fialho AM, Moreira LM, Granja AT, Popescu AO, Hoffmann K, Sa-Correia I (2008) Occurrence, production, and applications of gellan: current state and perspectives. Appl Microbiol Biotechnol 79(6):889–900. https://doi.org/10.1007/s00253-008-1496-0

Fulekar M, Sharma J (2008) Bioinformatics applied in bioremediation. Innov Rom Food Biotechnol 3:28

Gibson DT (1984) Microbial degradation of aromatic hydrocabons. Microb Degrad Org Compd 31:181–252

Johnsen AR, Karlson U (2005) PAH degradation capacity of soil microbial communities–does it depend on PAH exposure? Microb Ecol 50(4):488–495

Jouanneau Y, Micoud J, Meyer C (2007) Purification and characterization of a three-component salicylate 1-hydroxylase from *Sphingomonas* sp. strain CHY-1. Appl Environ Microbiol 73(23):7515–7521

Khara P, Roy M, Chakraborty J, Ghosal D, Dutta TK (2014) Functional characterization of diverse ring-hydroxylating oxygenases and induction of complex aromatic catabolic gene clusters in *Sphingobium* sp. PNB FEBS Open Bio 4:290–300

Pao SS, Paulsen IT, Saier MH (1998) Major facilitator superfamily. Microbiol Mol Biol Rev 62(1):1–34

Peng RH, Xiong AS, Xue Y, Fu XY, Gao F, Zhao W, Tian YS, Yao QH (2008) Microbial biodegradation of polyaromatic hydrocarbons. FEMS Microbiol Rev 32(6):927–955

Perez Vidakovics ML, Paba J, Lamberti Y, Ricart CA, Valle de Sousa M, Rodriguez ME (2007) Profiling the *Bordetella pertussis* proteome during iron starvation. J Proteome Res 6(7):2518–2528

Pieper DH, Reineke W (2000) Engineering bacteria for bioremediation. Curr Opin Biotechnol 11(3):262–270

Romine MF, Stillwell LC, Wong K-K, Thurston SJ, Sisk EC, Sensen C, Gaasterland T, Fredrickson JK, Saffer JD (1999) Complete sequence of a 184-kilobase catabolic plasmid from *Sphingomonas aromaticivorans* F199. J Bacteriol 181(5):1585–1602

Rutherford K, Parkhill J, Crook J, Horsnell T, Rice P, Rajandream M-A, Barrell B (2000) Artemis: sequence visualization and annotation. Bioinformatics 16:944–945

Sanchez J-C, Hochstrasser D, Rabilloud T (1999) In-gel sample rehydration of immobilized pH gradient. In: Link AJ (ed) 2-D proteome analysis protocols. Humana Press, Totowa, pp 221–225

Stolz A (2009) Molecular characteristics of xenobiotic-degrading sphingomonads. Appl Microbiol Biotechnol 81(5):793–811

Story S, Kline E, Hughes T, Riley M, Hayasaka S (2004) Degradation of aromatic hydrocarbons by *Sphingomonas paucimobilis* strain EPA505. Arch Environ Contam Toxicol 47(2):168–176

Tritt A, Eisen JA, Facciotti MT, Darling AE (2012) An integrated pipeline for de novo assembly of microbial genomes. PLoS ONE 7:e42304

Vandermeer KD, Daugulis AJ (2007) Enhanced degradation of a mixture of polycyclic aromatic hydrocarbons by a defined microbial consortium in a two-phase partitioning bioreactor. Biodegradation 18(2):211–221

Vandermeersch G, Lourenco HM, Alvarez-Munoz D, Cunha S, Diogene J, Cano-Sancho G, Sloth JJ, Kwadijk C, Barcelo D, Allegaert W, Bekaert K, Fernandes JO, Marques A, Robbens J (2015) Environmental contaminants of emerging concern in seafood—European database on contaminant levels. Environ Res 143:29–45

Waigi MG, Kang F, Goikavi C, Ling W, Gao Y (2015) Phenanthrene biodegradation by sphingomonads and its application in the contaminated soils and sediments: a review. Int Biodeterior Biodegrad 104:333–349

Xia Y, Min H, Rao G, Lv Z-m, Liu J, Ye Y-f, Duan X-j (2005) Isolation and characterization of phenanthrene-degrading *Sphingomonas paucimobilis* strain ZX4. Biodegradation 16(5):393–402

Yuan SY, Wei SH, Chang BV (2000) Biodegradation of polycyclic aromatic hydrocarbons by a mixed culture. Chemosphere 41(9):1463–1468

Zafra G, Absalón ÁE, Anducho-Reyes M, Fernandez FJ, Cortés-Espinosa DV (2017) Construction of PAH-degrading mixed microbial consortia by induced selection in soil. Chemosphere 172:120–126

Zhang H, Wang DZ, Xie ZX, Zhang SF, Wang MH, Lin L (2015) Comparative proteomics reveals highly and differentially expressed proteins in field-collected and laboratory-cultured blooming cells of the diatom *Skeletonema costatum*. Environ Microbiol 17:3976–3991

Zhao HP, Wang L, Ren JR, Li Z, Li M, Gao HW (2008) Isolation and characterization of phenanthrene-degrading strains *Sphingomonas* sp. ZP1 and Tistrella sp. ZP5. J Hazard Mater 152(3):1293–1300

Zhao Q, Hu H, Wang W, Peng H, Zhang X (2015) Genome sequence of *Sphingobium yanoikuyae* B1, a polycyclic aromatic hydrocarbon-degrading strain. Genome Announc 3(1):e01522–e01514

Zhao Q, Yue S, Bilal M, Hu H, Wang W, Zhang X (2017) Comparative genomic analysis of 26 *Sphingomonas* and *Sphingobium* strains: dissemination of bioremediation capabilities, biodegradation potential and horizontal gene transfer. Sci Total Environ 609:1238–1247